

## A monitoring system for mountain glaciers and ice caps using 30 meter resolution satellite data

Kazunari Nakano<sup>1</sup>, Yong Zhang<sup>1</sup>, Yoshihiro Shibuo<sup>2</sup>, Hironori Yabuki<sup>3</sup> and Yukiko Hirabayashi<sup>1</sup>

<sup>1</sup>Institute of Engineering Innovation, School of Engineering, the University of Tokyo, Japan

<sup>2</sup>Earth Observation Data Integration & Fusion Research Institute, School of Engineering, the University of Tokyo, Japan

<sup>3</sup>Japan Agency for Marine-earth Science and Technology, Japan

### Abstract:

We developed a monitoring system for deriving outlines of mountain glaciers and ice caps (MG&IC) at a 30 m horizontal resolution from Landsat Thematic Mapper (TM) and Landsat Enhanced Thematic Mapper plus (ETM+). Location and area information at 30 m resolution was obtained using a band ratio (TM4/TM5) and a threshold value of TM3 with a 9 by 9 pixel average filter. The total area and number of MG&IC were 449482 km<sup>2</sup> and 414258, respectively. The glacier outlines were similar to previous satellite-derived products for different regions. Although the derived glacier area was similar to previous estimates at regional scales, it was overestimated in some parts of Scandinavia where available satellite images are limited and only snowy season images can be used, and was underestimated in the western Himalayas and Caucasus where the glacier outlines are derived with difficulty from satellite images because of the effect of debris cover. Our system to monitor MG&IC has potential application in global hydrological and land-surface models and estimates of global sea-level rise.

KEYWORDS glacier outlines; satellite monitoring; Landsat; global

### INTRODUCTION

Loss of volume in mountain glaciers and ice caps (MG&IC) has been reported around the world in response to atmospheric warming (IPCC, 2007), significantly affecting terrestrial water resources (Immerzeel *et al.*, 2010; Kaser *et al.*, 2010) and contributing to global sea-level rise (Rignot *et al.*, 2003; Radić and Hock, 2010; Church *et al.*, 2011). To calculate current and future changes in glacier volumes, one of the most important data sets is a complete global glacier inventory with topographic attributes (e.g., minimum and maximum elevation, slope and aspect) for each glacier. However, recent calculations of sea-level rise due to MG&IC melting relied on estimates of the total volume of land ice scaled up from incomplete glacier inventories (e.g., Radić and Hock, 2010; Mernild *et al.*, 2011). Hence, a globally complete and detailed glaciological data set is urgently required.

The World Glacier Inventory (WGI) compiled informa-

tion on MG&IC from aerial photography, map and satellite imagery acquired during the 1960s and 1970s (WGMS, 1989). However, the WGI is not complete with respect to detailed glaciological information; only about 44% of MG&IC and 23% of their area are inventoried (Dyurgerov and Meier, 2005). Furthermore, the WGI makes change detection for individual glaciers nearly impossible because glaciers in the WGI are represented by point data rather than glacier outlines (WGMS, 1989). For this reason, the Global Land Ice Measurements from Space (GLIMS) project was designed to generate a global survey of digital glacier outlines from satellite data (Raup *et al.*, 2007; Armstrong *et al.*, 2012). To date the GLIMS Glacier Database, hosted at the National Snow and Ice Data Center (NSIDC) in Boulder, CO, USA, contains records for over 96792 glaciers with a total area of 325968 km<sup>2</sup> (Armstrong *et al.*, 2012). Although glacier inventories for British Columbia, Caucasus, Heard Island, Iceland, Irian Jaya, and Switzerland are complete in the GLIMS Glacier Database, the inventories for other regions are not yet completed. Further, some inventoried glaciers in the GLIMS Glacier Database are lacking topographic parameters and some data are based on somewhat old maps (Armstrong *et al.*, 2012). In addition, Cogley (2010) compiled an extended version of the WGI, called WGI-XF, through compilation of existing inventories including several older regional inventories that have been documented in WGMS (1989) but not in the WGI, and new inventories in Canada and the Sub-Antarctic. The WGI-XF contains records for over 131000 glaciers, covering approximately half of the MG&IC area (Cogley, 2010). Although glacier outlines can be derived from multispectral satellite data (e.g., Bayr *et al.*, 1994; Sidjak and Wheate, 1999; Paul and Andreassen, 2009), these studies mainly focused on regional scales. Such studies allow estimation of the fluctuations in glacier volumes in these regions, but are insufficient for estimating global changes. A globally complete inventory of glacier outlines, the Randolph Glacier Inventory (RGI) has been published recently (Arendt *et al.*, 2012). RGI primarily contains glacier outlines with little additional metadata for each record, and does not give the exact date of the determination of all glacier outlines. There is no question that global glacier outlines in different time series rather than snapshot and with date information are valuable.

Here we present a developed semi-automatic system to derive outlines of MG&IC (excluding glaciers in Greenland

Correspondence to: Yong Zhang, Institute of Engineering Innovation, School of Engineering, the University of Tokyo, 2-11-16 Yayoi, Bunkyo-ku, Tokyo 113-8656, Japan. E-mail: zhyong@sogo.t.u-tokyo.ac.jp ©2013, Japan Society for Hydrology and Water Resources.

Received 29 May, 2013  
Accepted 13 August, 2013

and Antarctica) from global satellite data with 30 m horizontal resolution. The system consists of semi-automatic data archiving and an automated mapping system running in a Linux/UNIX system. With the automated mapping system, our data set can be updated as new satellite data become available and will form a time series of glacier outlines, rather than a snapshot of location and extent. Furthermore, apart from enhancing glacier inventories for regions where few direct measurements exist, the 30 m global database of MG&IC, could be integrated into global hydrological and land-surface models.

## DATA

### *Satellite data*

Landsat TM and Landsat ETM+ images were provided in an orthorectified version (UTM projection, WGS84 datum) by the Global Land Cover Facility (GLCF). The images were selected with as low snow and cloud cover as possible to be suitable for glacier mapping. Each image covers 185 km × 185 km and contains reflection intensity information for each band. Satellite images including the locations of MG&IC obtained from Hirabayashi *et al.* (2010) or the GLIMS Glacier Data were analyzed. Overall, we selected 334 Landsat TM images acquired during 1985–1997 and 415 ETM+ images acquired during 1999–2003.

### *ASTER GDEM*

Specific topographic inventory parameters such as minimum, maximum, mean, and median elevation, mean slope, and mean aspect derived from a digital elevation model (DEM) were used for analysis of the obtained glacier outlines. For this study the Advanced Spaceborne Thermal Emission and Reflection Radiometer (ASTER) Global Digital Elevation Model (GDEM) with a horizontal resolution of 1 arc-second (~30 m) was used. It was released in July 2009 by the Ministry of Economy, Trade and Industry (METI), Japan, and NASA, covering the earth's surface between 83°N and 83°S.

As recent studies focusing on comparing a pre-release version of the ASTER GDEM and the DEM from the Shuttle Radar Topography Mission (SRTM) have shown (Hayakawa *et al.*, 2008; Frey and Paul 2012), the ASTER GDEM has higher resolution, fewer missing data, and better topographic representation than the SRTM DEM, particularly in high

mountainous areas with steep slopes. A report about typical artifacts and errors in the ASTER GDEM is given in METI/NASA/USGS (2009), which indicates that the overall accuracy of the global ASTER GDEM can be taken to be approximately 20 m at 95% confidence interval, which is adequate for deriving glacier details for our global inventory.

### *Glacier inventory data*

Glacier area on a continental scale from Radić and Hock (2010), the WGI-XF and the RGI were used to validate our estimate in each region (Table I). Radić and Hock (2010) calculated total glacierized area per region with complete glacier inventory from the WGI-XF data set and with incomplete glacier inventory from a global grid cell of glacierized area data set. The WGI-XF is an extended version of the WGI, in which a set of explicit specifications has been used to enhance the usefulness of the WGI data by eliminating low-level inconsistencies (Cogley, 2010). The RGI contains 170000 glacier outlines, which is a combination of both new and existing published glacier outlines (Arendt *et al.*, 2012). In addition, glacier inventories for British Columbia, Caucasus, Switzerland, and the eastern and western sides of the Himalayas (excluding India and Pakistan) are complete in the GLIMS Glacier Database, and were used to further evaluate our estimates.

## METHODS

### *Mapping of MG&IC*

Among methods for automated glacier mapping from multispectral satellite data, the band ratio method is considered the most efficient and convenient method (Paul, 2002; Raup *et al.*, 2007; Paul and Andreassen, 2009). It involves creating a thresholded ratio image from the raw digital numbers of bands TM3 (0.63–0.69 μm) or TM4 (0.76–0.90 μm) and TM5 (1.55–1.75 μm), relying on the spectral contrast between ice and snow and other surfaces. As expected from the spectral properties, glacier ice has a moderate reflectivity in the TM4 band (fine-grained snow has high reflectance) and very low reflectance in the TM5 band. The division of TM4 by TM5 yields high and consistent values over ice and snow, and very low values for the surrounding terrain. The glaciers can be therefore distinguished from other surface types where the TM4/TM5 ratio is larger than 3.6 (Supplement Figure S1). Because of

Table I. Total area of MG&IC in each region from the study of Radić and Hock (2010) (RH10), the WGI-XF (Cogley, 2010), the RGI (Arendt *et al.*, 2012), and estimates from this study.

Region	WGI-XF (km <sup>2</sup> )	RH10 (km <sup>2</sup> )	RGI (km <sup>2</sup> )	Area of this study (km <sup>2</sup> )	Number of this study
North America	29,879	100,740	104,315	114,792	76,420
South America	20,649	36,700	38,135	51,904	31,217
Iceland	11,005	11,005	11,060	16,387	31,217
Central Europe	3,045	3,045	2,064	2,825	3,259
Caucasus	1,397	1,397	1,354	1,595	2,709
High Mountain Asia	107,340	114,330	64,524	191,622	193,191
New Zealand	1,156	1,156	1,162	1,921	2,456
Scandinavia	3,057	3,057	2,853	38,201	46,018
North and East Asia	2,902	2,902	2,933	27,572	27,771
Total	180,430	274,332	228,400	446,819	414,258

spectral similarity with the surrounding terrain, some non-glacier areas at the edge of the image were identified as glaciers after applying the threshold  $TM4/TM5 > 3.6$  (Supplement Figure S2). Also, some forested areas were identified as glaciers (Supplement Figure S2b). Hence, an additional threshold of  $TM3 (DN > 50)$  was applied to improve glacier mapping, exploiting the very high reflectivity of ice and snow in the  $TM3$  band. The errors at the edge of the image were removed after applying the additional threshold in  $TM3$  (Supplement Figure S2c). As a last step of the main processing, a  $9 \times 9$  pixel average filter was applied to remove misclassification of pixels and noise, i.e. to eliminate isolated pixels and fill small gaps in glacier-covered regions (Supplement Figure S3). Finally, outlines of glaciers were obtained as an individual mass of contiguous glacier pixels. See Supplement Information S1 for the details.

### Topographic information

Satellite-derived glacier outlines combined with the ASTER GDEM were used to derive topographic parameters for analyzing the glaciers, which include hypsometry, maximum, minimum and mean elevations. Note that the ASTER GDEM is the same spatial resolution as Landsat data (30 m), and also uses the same UTM coordinate system. However there are still some points that do not match between the two datasets. Although it is necessary to develop a mosaic from different scenes from different years, our study aimed to extract glacier outlines globally, and does not focus on the point or small catchment scale. This makes matching these points more difficult globally; hence we did not match them in the edges of imageries. As previous studies suggested (e.g., Frey and Paul, 2012; Hebel and Purves, 2009), although some grid points that may have an influence on the hypsography of small glaciers are not equal to each other, local differences in these data have only a small influence on the hypsography of large glaciers.

## RESULTS

In total, 414258 mapped glaciers with a total area of 449482 km<sup>2</sup> were identified in the 30 m global glacier database (Supplement Figure S4). Of all the regions defined (Table I), High Mountain Asia contains the largest ice mass outside of Antarctica and Greenland, representing ~42.6% of the total area of MG&IC, while the area in the Caucasus, Central Europe and New Zealand is relatively small, representing less than 1% of the total area.

The distribution of glacier area with elevation in Central Europe, the Caucasus, the Himalayas, North America and South America is depicted in Figure 1. Most of the glacier area occurs between 4500 m and 6000 m a.s.l. in the Himalayas, and glaciers in Central Europe and the Caucasus are distributed mainly in the altitudinal range of 2000 to 4000 m a.s.l. (Figure 1). In North America and South America, the elevation of most glaciers is relatively low, about 1500 m a.s.l., and some ice is also found between 3000 m and 5000 m a.s.l. (Figure 1).

The glaciers of each region are classified into size bins, and the total area per size bin is determined. Similar to previous studies (e.g., Raper and Braithwaite, 2005; Radić

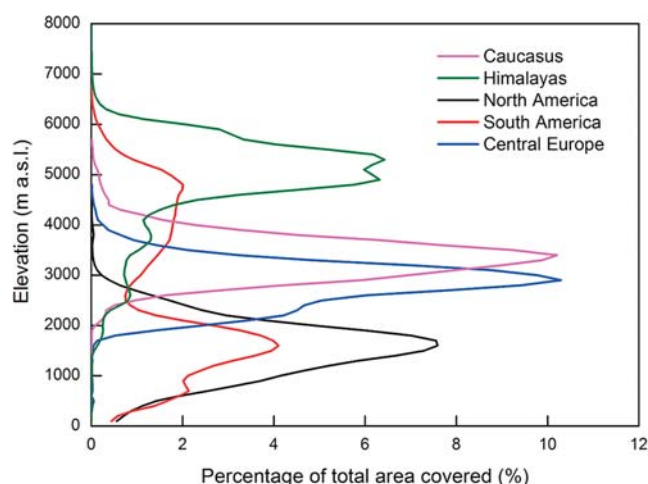


Figure 1. Glacier area-elevation distribution in the Caucasus, Himalayas, Central Europe, North America and South America in 100 m elevation bins

and Hock, 2010) we assign the upper boundaries for each area size bin to be  $2^n$  km<sup>2</sup> with  $n$  ranging from  $-3$  to  $15$ . This means that the smallest size bin contains glaciers of less than 0.125 km<sup>2</sup> while the largest size bin contains glaciers between 16384 km<sup>2</sup> and 32768 km<sup>2</sup>. The cumulative number distribution of MG&IC for each size bin in Central Europe, the Caucasus, High Mountain Asia, North America and South America is shown in Figure 2. Our estimates were larger than those in the WGI-XF (Figure 2). Note that the WGI-XF does not cover all glaciers in these regions, and its average map year is 1964 with standard deviation of eleven years and a time range from 1901 to 1993 (Cogley, 2010; Radić and Hock, 2010), whereas our glacier database is derived from Landsat TM or ETM+ images acquired during recent decades. Furthermore, our results for small glaciers are more complete than other glacier inventories (e.g., WGMS, 1989; Cogley, 2010). In accordance with our estimation, small glaciers with area  $\leq 1$  km<sup>2</sup> in the Central Europe, Caucasus, High Mountain Asia, North America and South America account for 69% of the total number of MG&IC (Figure 2). Especially in High Mountain Asia small glaciers account for ~44% of the total number (Figure 2e).

## DISCUSSION

### Error assessment

The accuracy of the mapped glacier outlines is an important but difficult topic in glacier mapping from satellite data (Raup *et al.*, 2007; Racoviteanu *et al.*, 2010), especially in regions with shadow, clouds, seasonal snow, proglacial lakes and debris cover. A comparison of glacier area from different databases indicated that the total area of MG&IC is fairly similar to previous estimates with the exception of Scandinavia and North and East Asia (Table I). Although images were selected with acquisition dates prior to the onset of heavy snowfall (approximately October 1 in the Northern Hemisphere and April 1 in the Southern Hemisphere) as late in the melt season as possible, only a few satellite images are acquired in May or June in

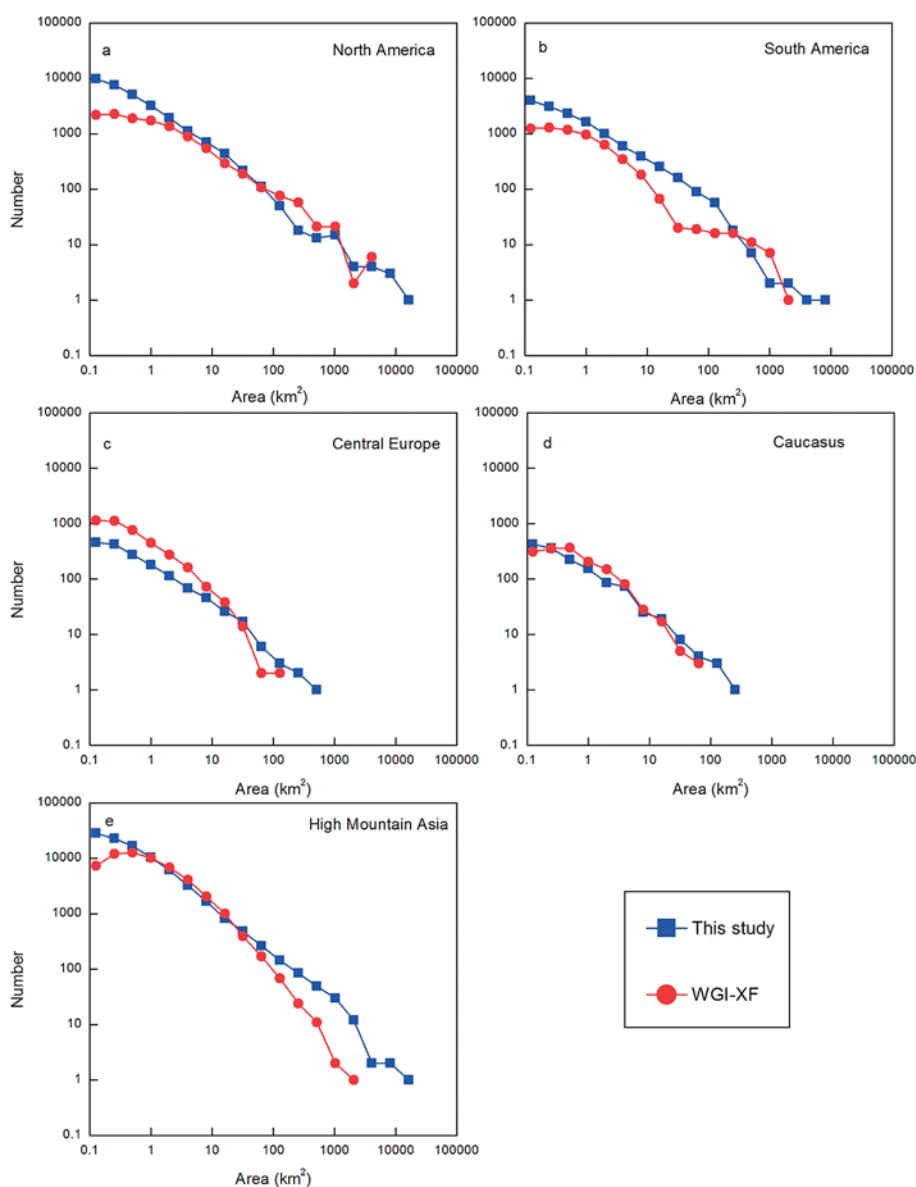


Figure 2. Cumulative number of glaciers for each size bin in (a) North America, (b) South America, (c) Central Europe, (d) the Caucasus, and (e) High Mountain Asia. Blue and red colours denote our glacier database and the WGI-XF inventory

Scandinavia and North and East Asia. Consequently, seasonal snow may be identified as glacier pixels, resulting in overestimation in these regions. The relatively simple assumption of the onset of snowfall may lead to the overestimation of glacier area where snow season is out of the assumed periods, such as in the low latitude regions of the Southern Hemisphere where dry season is from May to August (Sicart *et al.*, 2011). In addition, the area of debris-covered glaciers was underestimated in the western Himalaya and Caucasus where debris-covered areas are large, and are excluded from glacier area by this method. Although several methods for debris-cover mapping have been applied to different debris-covered glaciers (e.g., Bishop *et al.*, 2000; Paul *et al.*, 2004a; Racoviteanu *et al.*, 2010), there is no single best method for debris-cover mapping that can be applied to large regions without some manual corrections of the resulting outlines. Combination

of our method and state-of-the-art techniques to extract spatial distribution of debris using satellite information (e.g., Zhang *et al.*, 2011) may improve our inventory over debris-covered glaciers.

The method used in this study is efficient in delineating clean ice in a timely manner, but might not work properly for ice in shadow. Ice in shadow needs to be delineated manually or using algorithms customized and tested for such cases (Racoviteanu *et al.*, 2010). In addition, we applied a  $9 \times 9$  pixel average filter to remove misclassification of pixels and noise, i.e. to eliminate isolated pixels and fill small gaps in glacier-covered regions, with the consequence that this process maybe lead to an underestimate of the area of small glaciers.

#### *Area-altitude distribution for MG&IC*

The altitude distribution as a function of area for glaciers

Table II. Average correlations of the glacier area-altitude distribution between this study and the models assumed shaped distributions for each glacier.

	Central Europe	Caucasus	Himalayas	North America	South America
1/3 shifted normal distribution	0.64	0.65	0.63	0.40	0.30
Triangle distribution	0.76	0.76	0.75	0.46	0.38

has been modelled in previous studies to estimate glacier mass balance according to altitude (e.g., Raper *et al.*, 2000; Paul *et al.*, 2004b; Raper and Braithwaite, 2006; Hirabayashi *et al.*, 2010). Because of limited hypsometric data for glaciers, these studies assumed relatively simple shapes to estimate the area-altitude distribution of glaciers. Raper *et al.* (2000) and Raper and Braithwaite (2006) assumed a linearly increasing function from the terminus to mean altitude and a linearly decreasing function above that altitude to approximate the area-altitude distribution (hereafter called the Triangle distribution). Hirabayashi *et al.* (2010) assumed that the altitude distribution of a glacier has a normal distribution curve that is shifted by one third of the range between the maximum and minimum altitudes. We evaluated the existing area-altitude models using our glacier database by calculating correlations for our estimate and the two area-altitude assumptions (the Triangle distribution and 1/3 shifted normal distribution) for each 50 m altitude interval (Supplement Figure S5). The altitude distribution was obtained for the entirety of each glacier. The average correlations between the altitude distribution of glaciers and each assumed shape distribution in Central Europe, the Caucasus, the Himalayas, North America and South America shows that correlations are low in North America and South America (Table II). Overall, there is a better match with the Triangle distribution than with the 1/3 shifted normal distribution in these regions (Table II).

## CONCLUSIONS

A 30 m global outline of MG&IC was derived from Landsat TM and ETM+ images, which are available for immediate use. Our database contains records for over 414258 glaciers with a total area of 449482 km<sup>2</sup>. Although there are errors due to limitations in satellite images and applied methods in some regions such as Scandinavia, North and East Asia, and the western Himalayas and Caucasus, our database matches well with previous satellite-derived estimates at regional scales, which is the appropriate scale needed for monitoring future fluctuations in MG&IC. Evaluation of published area-altitude models showed that the Triangle distribution resembles those obtained from our database in the Alps, the Caucasus, and the Himalayas. In particular, the developed 30 m glacier outlines can easily connect with other gridded data such as temperature or precipitation data to aid in the development of land surface modelling. We expect that our glacier outlines, which can be updated from recent satellite record in a semi-automatic way, can be used for a wide range of scientific purposes.

## ACKNOWLEDGEMENTS

The research was supported by funding programs for next-generation world-leading researchers by the Japan Society for the Promotion of Science (JSPS) and Core Research for Evolutional Science and Technology (CREST) project of the Japan Science and Technology Agency (JST).

## SUPPLEMENTS

Detail explanation of a method to extract glacier outline from Landsat TM/ETM+ images (Supplement Information S1, Supplement Figure S1, S2 and S3), spatial distribution of derived outlines of MG&IC (Supplement Figure S4) and an example of the area-altitudinal distribution for the glacier (Supplement Figure S5) are given in the supplementary materials.

## REFERENCES

- Arendt A, Bolch T, Cogley JG, Gardner A, Hagen J-O, Hock R, Kaser G, Pfeffer WT, Moholdt G, Paul F, Radić V, Andreassen L, Bajracharya S, Beedle M, Berthier E, Bhambri R, Bliss A, Brown I, Burgess E, Burgess D, Cawkwell F, Chinn T, Copland L, Davies B, de Angelis H, Dolgova E, Filbert K, Forester R, Fountain A, Frey H, Giffen B, Glasser N, Gurney S, Hagg W, Hall D, Haritashya UK, Hartmann G, Helm C, Herreid S, Howat I, Kapustin G, Khromova T, Kienholz C, Koenig M, Kohler J, Kriegel D, Kutuzov S, Lavrentiev I, LeBris R, Lund J, Manley W, Mayer C, Miles E, Li X, Menounos B, Mercer A, Moelg N, Mool P, Nosenko G, Negrete A, Nuth C, Pettersson R, Racoviteanu A, Ranzi R, Rastner P, Rau F, Rich J, Rott H, Schneider C, Seliverstov Y, Sharp M, Sigursson O, Stokes C, Wheate R, Winsvold S, Wolken G, Wyatt F, Zhelty-hina N. 2012. Randolph Glacier Inventory [v20]: A Dataset of Global Glacier Outlines Global Land Ice Measurements from Space, Boulder Colorado, USA, Digital Media (with area corrections downloaded 2012).
- Armstrong R, Raup B, Khalsa SJS, Barry R, Kargel J, Helm C, Kieffer H. 2012. GLIMS glacier database. Boulder, Colorado USA: National Snow and Ice Data Center, Digital media.
- Bayr K, Hall D, Kovalick W. 1994. Observations on glaciers in the eastern Austrian Alps using satellite data. *International Journal of Remote Sensing* **15**: 1733–1742. doi: 10.1080/01431169408954205.
- Bishop MP, Kargel JS, Kieffer HH, MacKinnon DJ, Raup BH, Shroder Jr JF. 2000. Remote-sensing science and technology for studying glacier processes in high Asia. *Annals of Glaciology* **31**: 164–170. doi: 10.3189/172756400781820147.
- Church JA, White NJ, Konikow LF, Domingues CM, Cogley JG, Rignot E, Gregory JM, van den Broeke MR, Monaghan AJ, Velicogna I. 2011. Revisiting the Earth's sea-level and energy budgets from 1961 to 2008. *Geophysical Research Letters* **38**: L18601. doi: 10.1029/2011GL048794.

- Cogley JG. 2010. A more complete version of the World Glacier Inventory. *Annals of Glaciology* **50**: 32–38. doi: 10.3189/172756410790595859.
- Dyrurgerov MB, Meier MF. 2005. Glaciers and the changing earth system: a 2004 snapshot. Occasional Paper 58, Institute of Arctic and Alpine Research, University of Colorado at Boulder, Boulder, Colorado, USA.
- Frey H, Paul F. 2012. On the suitability of the SRTM DEM and ASTER GDEM for the compilation of topographic parameters in glacier inventories. *International Journal of Applied Earth Observation and Geoinformation* **18**: 480–490. doi: 10.1016/j.jag.2011.09.020.
- Hayakawa YS, Oguchi T, Lin Z. 2008. Comparison of new and existing global digital elevation models: ASTER G-DEM and SRTM-3. *Geophysical Research Letters* **35**: L17404. doi: 10.1029/2008GL035036.
- Hebeler F, Purves RS. 2009. The influence of elevation uncertainty on derivation of topographic indices. *Geomorphology* **111**: 4–16. doi: 10.1016/j.geomorph.2007.06.026.
- Hirabayashi Y, Döll P, Kanae S. 2010. Global-scale modeling of glacier mass balances for water resources assessments: Glacier mass changes between 1948 and 2006. *Journal of Hydrology* **390**: 245–256. doi: 10.1016/j.jhydrol.2010.07.001.
- Immerzeel WW, van Beek LPH, Bierkens MFP. 2010. Climate Change Will Affect the Asian Water Towers. *Science* **328**: 1382–1385. doi: 10.1126/science.1183188.
- Intergovernmental Panel on Climate Change (IPCC). 2007. Climate Change: The physical science basis. Contribution of Working Group I to the fourth assessment report of the intergovernmental panel on climate change, Cambridge University Press, Cambridge, UK.
- Kaser G, Grosshauser M, Marzeion BC. 2010. Contribution potential of glaciers to water availability in different climate regimes. *Proceedings of the National Academy of Sciences of the United States of America* **107**: 20223–20227. doi: 10.1073/pnas.1008162107.
- Mernild S, Liston G, Hiemstra C, Christensen J, Stendel M, Hasholt B. 2011. Surface Mass Balance and Runoff Modeling Using HIRHAM4 RCM at Kangerlussuaq (Søndre Stromfjord), West Greenland, 1950–2080. *Journal of Climate* **24**: 609–623. doi: 10.1175/2010JCLI3560.1.
- METI/NASA/USGS. 2009. ASTER GDEM Validation. Summary Report, 28 pp.
- Paul F. 2002. Changes in glacial area in Tyrol, Austria, between 1969 and 1992 derived from Landsat 5 thematic mapper and Austrian Glacier Inventory data. *International Journal of Remote Sensing* **23**: 787–799. doi: 10.1080/01431160110070708.
- Paul F, Andreassen L. 2009. A new glacier inventory for the Svartisen region, Norway, from Landsat ETM plus data: challenges and change assessment. *Journal of Glaciology* **55**: 607–618. doi: 10.3189/002214309789471003.
- Paul F, Huggel C, Kääb A. 2004a. Combining satellite multispectral image data and a digital elevation model for mapping debris-covered glaciers. *Remote Sensing of Environment* **89**: 510–518. doi: 10.1016/j.rse.2003.11.007.
- Paul F, Kääb A, Maisch M, Kellenberger T, Haeberli W. 2004b. Rapid disintegration of Alpine glaciers observed with satellite data. *Geophysical Research Letters* **31**: L21402. doi: 10.1029/2004GL020816.
- Racoviteanu AE, Paul F, Raup B, Khalsa SHS, Armstrong R. 2010. Challenges and recommendations in mapping of glacier parameters from space: results of the 2008 Global Land Ice Measurements from Space (GLIMS) workshop, Boulder, Colorado, USA. *Annals of Glaciology* **50**: 53–69. doi: 10.3189/172756410790595804.
- Radić V, Hock R. 2010. Regional and global volumes of glaciers derived from statistical upscaling of glacier inventory data. *Journal of Geophysical Research* **115**: F01010. doi: 10.1029/2009JF001373.
- Raper SCB, Braithwaite RJ. 2005. The potential for sea level rise: New estimates from glacier and ice cap area and volume distributions. *Geophysical Research Letters* **32**: L05502. doi: 10.1029/2004GL021981.
- Raper SCB, Braithwaite RJ. 2006. Low sea level rise projections from mountain glaciers and icecaps under global warming. *Nature* **439**: 311–313. doi: 10.1038/nature04448.
- Raper SCB, Brown O, Braithwaite RJ. 2000. A geometric glacier model for sea-level change calculations. *Journal of Glaciology* **46**: 357–368. doi: 10.3189/172756500781833034.
- Raup B, Kääb A, Kargel JS, Bishop MP, Hamilton G, Lee E, Paul F, Rau F, Soltes D, Khalsa SJS, Beedle M, Helm C. 2007. Remote sensing and GIS technology in the Global Land Ice Measurements from Space (GLIMS) Project. *Computers & Geosciences* **33**: 104–125. doi: 10.1016/j.cageo.2006.05.015.
- Rignot E, Rivera A, Casassa G. 2003. Contribution of the Patagonian icefields of South America to sea level rise. *Science* **302**: 434–437. doi: 10.1126/science.1087393.
- Sicart JE, Hock R, Ribstein R, Litt M, Ramirez E. 2011. Analysis of seasonal variations in mass balance and meltwater discharge of the tropical Zongo Glacier by application of a distributed energy balance model. *Journal of Geophysical Research* **116**: D13105. doi: 10.1029/2010JD015105.
- Sidjak R, Wheate R. 1999. Glacier mapping of the Illecillewaet icefield, British Columbia, Canada, using Landsat TM and digital elevation data. *International Journal of Remote Sensing* **20**: 273–284. doi: 10.1080/014311699213442.
- WGMS (World Glacier Monitoring Service). 1989. World glacier inventory: status 1988. IAHS(ICS)/UNEP/UNESCO, World Glacier Monitoring Service, Zürich.
- Zhang Y, Fujita K, Liu S, Liu Q, Nuimura T. 2011. Distribution of debris thickness and its effect on ice melt at Hailuoguo glacier, southeastern Tibetan Plateau, using in situ surveys and ASTER imagery. *Journal of Glaciology* **57**: 1147–1157. doi: 10.3189/002214311798843331.